Decolourization of Cationic and Anionic Dyes from Aqueous Solution by Adsorption on NaOH Treated Eggshells: Batch and Fixed Bed Column Study using Response Surface Methodology

S. Akazdam[1], M. Chafi[1], W. Yassine[1], L. Sebbahi[1], B. Gourich[1], N. Barka[2]

[1]. Laboratory of Engineering, Processes and Environment (LEPE) High School of Technology, University Hassan II of Casablanca Morocco.
[2]. University Hassan 1, Laboratoire des Sciences des Matériaux, des Milieux et de la Modélisation (LS3M), BP.145, 25000 Khouribga, Morocco.

Abstract

In this study, we investigated the adsorption of Methylene blue (MB) and Acid Orange 7 (AO7) dyes on a natural adsorbent, we have selected a food derivative product (eggshells) treated with NaOH (TES) as a new and potential biosorbent. Different models of adsorption isotherms in batch study were applied to fit experimental equilibrium data at different solution temperatures; Langmuir and Temkin model fitted the adsorption data quite reasonably ($R^2 > 0.98$). Results have showed that the adsorption of MB on TES dye followed very well the second order kinetic model. The thermodynamic parameters were evaluated; the negative values of $\Delta H°$ and $\Delta G°$ indicated respectively that the adsorption of MB onto TES was exothermic and spontaneous process. The continuous method was modeled by response surface methodology (RSM) . The effect of operating parameters such as flow rate, initial dye concentration, and bed height were exploited in this study. The precision of the equation obtained by Box–Behnken design (BBD) utility for modeling and optimization by response surface methodology RSM was confirmed by the analysis of variance (ANOVA). The optimum conditions proposed by Box–Behnken design (BBD) to reach the maximum dye removal through adsorption process. Under the optimum conditions, the removal efficiency ofAO7 was 89.89%. In summary, the results have established good potentiality for the waste eggshell particles to be used as a sorbent for the removal of MB from wastewater in batch study and were shown to be suitable adsorbent for adsorption of AO7 using fixed-bed adsorption column.

1. Introduction

It is undeniable that our planet suffers from a problem that is becoming dangerous which is linked to a possible water shortage in the coming days. On the other hand, with technological advances and population growth, water demand has increased. The degree of pollution becomes more and more pronounced because of effluents and emissions released from different industries. Dyes sectors, printing and finishing of textiles occupy a special place because these activities generate significant wastewater pollution with warning qualitative and quantitative amounts of several types of pollutants that may be acidic or basic dyes in nature [1].

Dyes are one of the important classes of the pollutants whose presence in water bodies is toxic to aquatic as well as human lives, this is due to the presence of an aromatic structure and, in some cases, metals in their structure. The biodegradability of this type of pollution is generally difficult because dyes have a synthetic origin and a complex molecular structure which makes them more stable and difficult to be biodegraded [2].

There are several methods that can be classified into two types: physical and chemical processes to treat water charged with dyes, but adsorption is considered now as one of the most important separation technologies insofar the adsorbent can be regenerated in part or completely for the another use. Activated carbon is the most commonly used adsorbent but it is very expensive which imposes the need for regeneration; this is why the development of adsorbent based on natural products and cheaper proves a very interesting solution, this technology is termed biosorption [3]. Lot of non-conventional low cost adsorbent such as rice hull ash, sugarcane bagasse, clay, durian shell, banana stalk waste and mango seed kernel powder, sawdust, pine needle, eucalyptus bark, prawn shell activated carbon, and mango seed kernel powder have been used for the removal of dyes and heavy metal ions from aqueous solution. In addition to their low cost, the use of bioadsorbent generates several other benefits for example is cited: good adsorption capacity, selective adsorption of effluent, free availability, easy regeneration and requires relatively simple technologies [4].

This study aims, among other things, minimization of MBand AO7 in aqueous solution and to promote this abundant material in our country by reusing it from waste of houses and restaurants. Eggshell is composed chemically of: 94 to 97% calcium carbonate; 3% to 6% protein; 1% of various minerals (including magnesium,

potassium and trace amounts of iron, sulfur and phosphorus) [5]. To increase its adsorption capacity, the eggshells were chemically treated by NaOH, indeed, this treatment is viewed as one of the widely used chemical treatment techniques for surface modification of agricultural waste for the purpose of improving its adsorption properties such as structural durability, reactivity and natural ion-exchange capacity [6]. Adsorption in batch study and fixed-bed columns using activated carbon has been widely used in industrial processes for the removal of contaminants from aqueous textile industry effluents, since it does not require the addition of chemical compounds in the separation process [7]. Adsorption in a fixed bed column can be used continuously under high effluent flow rates and it has been used in many pollution control processes such as removal of ions by an adsorbent bed or removal of toxic organic compounds by carbon adsorption [8]. In this study, the TES has been tested for removal of aqueous solutions. In application of adsorption process on an industrial scale, it is crucial to improve process efficiency, reduce operational cost and time to minimum and take into account the most important factors, what can be achieved by applying the optimization techniques such as response surface methodology (RSM). Determining the effect of a single factor on the efficiency of the process is relatively simple. It is definitely more of a challenge to assess the effect of several parameters at once. Response surface methodology based on experimental data makes easier to plan the entire modeling process by reducing the number of experiments to the necessary minimum, and allows a mathematical equation to fit the experimental results, which is required for the process optimization [9].

In our study, we were interested to the adsorption process of MB onto NaOH treated eggshell (TES). The experimental part of this study was based on modeling the adsorption kinetic, the verification of different adsorption isotherm and the estimation of thermodynamic properties in batch systems. In continuous system, TES is used to remove azo dye (AO7) from aqueous solution through column studies. The objective of this study was to investigate the adsorption potential of AO7 onto TES fixed-bed. The important design parameters such as inlet concentration of dye solution, fluid flow rate and column bed height [10] were investigated using a laboratory scale fixed-bed column. The main effects and interaction effects between process variables on the dye adsorptions were analyzed based on the BBD. Their maximum adsorption capacities have been optimized using RSM method.

2. Materials and methods
2.1. *Preparation and Characterization of Eggshell Powder*

Eggshell, were collected from houses and local restaurants. To remove impurity and adhering dirt, it were first washed several times in tap water, and then boiled in distilled water. The washed materials were then dried at 100°C for 24 h in the dry oven. The dried eggshells were crushed and sieve to recover the particle size powders between 0.250 and 0.711 mm. Finally, the sieved material was treated with sodium hydroxide NaOH 2N for 2 hin a flask heated with reflux, then the sample was washed until neutralization and dried in the oven at 100°C for 24 h. To remove moisture before each use, we put the resulting adsorbent TES in a dryer.Fourier Transform Infrared (FTIR) analysis was applied to determine the surface functional groups, using FTIR spectrophotometer (SCO TECH SP-FTIR-1). The spectra were recorded from 4000 to400 cm^{-1}[11].

2.2. *Adsorbate Preparation*
2.2.1. *Methyleneblue*
Methylene blue is a dye having the empirical formula $C_{16}H_{18}N_3S$, λ (665nm) and a molecular mass M=319.86g/mol; the molecular structure is represented in Fig.1. This organic dye is used to test the adsorption capacity of adsorbents and measure their surface areas. A stock solution was prepared by dissolving 0.5 g of dye in 1 liter of distilled water, and to prepare the desired concentrations are done dilutions [12].
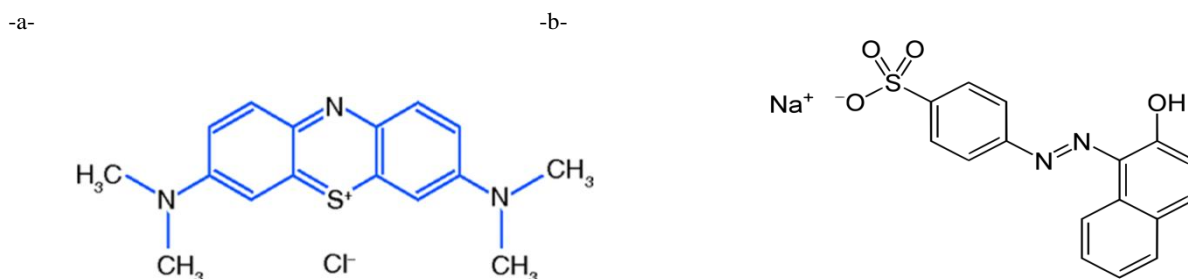

Fig. 1: Molecular structure of: -a- Methylene blue. −b- Acid Orange 7.

2.2.2. Acid Orange 7

The Acid Orange 7 dye also called Acid Orange II (Sigma-Aldrich), belonging to the family of the anionic dyes. AO7 is a dye having the empirical formula C16H11N2NaO4S, molecular mass 350.33 g/mol and λ (485nm). It is representative of a textile type of pollution. Its structural formula is shown in Fig.1. Stock solutions were prepared by dissolving requisite quantity of dye without further purification in distilled water, and the concentrations used were obtained by dilution of the stock solution. The pH was adjusted to a given value by addition of HCl (1N) or NaOH (1N) [13].

2.3. Biosorption Isotherms

The batch adsorption experiments were conducted in a set of 250 ml erlenmeyer flask containing adsorbent and 200 ml of MB solution at various initial concentrations. The flasks were agitated in an isothermal water-bath shaker at 200 rpm and solution temperature was varied in the range (25–35°C); All mixtures were studied until the equilibrium is reached. After decantation and centrifugation for 5min at 2000tr/min, the equilibrium concentrations of dye in the solution were measured at 665 nm. The pH of solutions was adjusted with 1N Hcl or 1N NaOH solutions [14].

2.4. Biosorption kinetics

The main objective of this kinetic study is to see the influence of several parameters on the law of speed contact time of the MB adsorption process on the TES such as temperature, initial dye concentration using the batch technique. In a batch reactor, we contacted a volume of 3L MB of solutions at different concentrations ranging from 5 to 100 ppm with a 3g TES mass maintaining a constant stirring speed and a definite temperature. At intervals of definite time, samples were taken, centrifuged for measuring the residual concentration by UV-visible spectrophotometer at λ = 665 nm. These experiments were conducted at varying temperatures values (20, 25, 30 and 35°C). The dye removal percentage was calculated [15] from:

$$R_e(\%) = 100 \; x \; \frac{(C_0 - C_e)}{C_0} \qquad (1)$$

Where C_0 is the initial concentration of dye in solution (mg/L), and C_e is the final dye concentration in aqueous solution after phase separation (mg/L). The amount of biosorption per gram of TES at any time t, q_t (mg/g), was evaluated using [16]:

$$q_t = (C_0 - C_t) \; x \; \frac{v}{m} \qquad (2)$$

Where C_0 and C_t (mg/L) are the liquid-phase concentrations of MB at initial and any time t respectively, v is the volume of the solution (L) and m is the TES mass (g).

2.5. Isotherm Modeling

The isothermal curves describe the relationship at the adsorption equilibrium between adsorbed specie and an adsorbent amount in a given solvent at a constant temperature. The adsorption isotherms were performed with different initial concentrations in order to determine the sorption mechanisms, the surface properties and affinities of the sorbent and the adsorption saturation capacity. A suitable model can be found by plotting solid phase concentration against liquid phase concentration graphically [17].Several models were analyzed such as Langmuir, Freundlich, Dubinin–Radushkevich (D–R), generalized isotherm and Temkin isotherm. Linear regression is frequently used to determine the best-fitting isotherm [18].The theoretical Langmuir sorption isotherm is valid for adsorption of a solute from a liquid solution as monolayer adsorption on a surface containing a finite number of identical sites. The model is based on several basic assumptions [19]:
1. Adsorption is assumed to take place at specific homogenous sites with the adsorbent;
2. Once a dye molecule occupies a site;
3. The adsorbent has a finite capacity for the adsorbate (at equilibrium);
4. All sites are identical and energetically equivalent.

Therefore, the Langmuir isotherm model was chosen for estimation of the maximum adsorption capacity corresponding to complete monolayer coverage on the sorbent surface. The generalized non-linear form of the Langmuir isotherm is represented by:

$$q_e = \frac{q_{max} K_L C_e}{1 + K_L C_e} \qquad (3)$$

Where C_e (mg/L) is the concentration of MB solution at equilibrium; q_e (mg/g) is the corresponding adsorption capacity; q_{max} is the Langmuir isotherm constant (maximum adsorption capacity) (mg/g); K_L is a constant related to the adsorption energy (L/mg).The linear equation of Langmuir isotherm model can be written as followed:

$$\frac{C_e}{q_e} = \frac{C_e}{q_{max}} + \frac{1}{K_L q_{max}} \qquad (4)$$

The essential characteristic of the Langmuir isotherm can be expressed by the dimensionless constant called equilibrium parameter R_L defined by [20]:

$$R_L = \frac{1}{1 + K_L C_0} \qquad (5)$$

The separation factor R_L values indicate the type of isotherm to be irreversible ($R_L = 0$), favorable ($0 < R_L < 1$), linear ($R_L = 1$) or unfavorable ($R_L > 1$).

The Freundlich isotherm model is the earliest known relationship describing the sorption process. The model applies to adsorption on heterogeneous surfaces with interaction between adsorbed molecules and the application of the Freundlich equation also suggests that sorption energy exponentially decreases on completion of the sorptional centers of an adsorbent. This isotherm is an empirical equation that can be employed to describe heterogeneous systems and is expressed as [21]:

$$q_e = K_F C_e^{1/n} \qquad (6)$$

Where K_F is the Freundlich constant related to the bonding energy. It can be defined as the adsorption or distribution coefficient and represents the quantity of dye adsorbed onto adsorbent for unit equilibrium concentration. 1/n is the heterogeneity factor and n parameter is a measure of the deviation from linearity of adsorption. Its value indicates the degree of non-linearity between solution concentration and adsorption as follows: if n=1, the adsorption is linear; if the value n< 1, this implies that adsorption process is chemical; if the value n>1, adsorption is a favorable as physical process. Conversely, the values of (1/n < 1) and (1/n>1) indicate a normal Langmuir and cooperative adsorption, respectively. Equation (6) can be linearized in the logarithmic form (7) so that the Freundlich constants can be determined:

$$\log(q_e) = \log(K_F) + \frac{\log(C_e)}{n} \qquad (7)$$

Temkin isotherm model contains a factor that explicitly takes into account adsorbing species–adsorbate interactions. This model assumes the following:

1. The heat of adsorption of all the molecules in the layer decreases linearly with coverage due to adsorbate–adsorbate interactions.

2. Adsorption is characterized by a uniform distribution of binding energies, up to some maximum binding energy. The derivation of the Temkin isotherm assumes that the fall in the heat of sorption is linear rather than logarithmic, as implied in the Freundlich equation.

The Temkin isotherm has commonly been applied in the following form [22] :

$$q_e = \frac{RT}{b_1} \ln(k_1 C_e) \qquad (8)$$

The Temkin isotherm can be expressed in its linear form as:

$$q_e = B_1 \ln(k_1) + B_1 \ln(C_e) \qquad (9)$$

$$B_1 = \frac{RT}{b_1} \qquad (10)$$

Where T is the absolute temperature in °K and R is the universal gas constant 8.314 J/(mol.°K). The constant b_1 is related to the heat of adsorption. The adsorption data were analyzed according to the linear form of the Temkin isotherm.

Another equation used in the analysis of isotherms was proposed by Dubinin–Radushkevich. D–R model was applied to estimate the porosity apparent free energy and the characteristic of adsorption. The D–R isotherm is not assuming a homogeneous surface or constant sorption potential but its common and linear forms can be [23]:

$$q_e = Q_{max} \exp(-K\varepsilon^2) \qquad (11)$$

And

$$\ln q_e = \ln Q_m - K\varepsilon^2 \qquad (12)$$

Where K is a constant related to the adsorption energy, Q_m the theoretical saturation capacity, ε is the Polanyi potential. ε can be calculated from (13):

$$\varepsilon = RT \ln(1 + \frac{1}{C_e}) \qquad (13)$$

The plot's slope of $\ln(q_e)$ versus ε^2 gives the constant K (mol^2/(kJ^2)) and the intercept yields to adsorption capacity, Q_m (mg/g). K gives the mean free energy of adsorption (E) per molecule of the sorbate when it is transferred to the surface of the solid from infinity in the solution and can be computed using [24]:

$$E = \frac{1}{\sqrt{2k}} \qquad (14)$$

The magnitude of E is useful for estimating the type of adsorption process. Adsorption type can be explained by chemical adsorption if the magnitude of E is 8–16 kJ/mol. It's accepted that when the adsorption energy is lower than 8 kJ/mol, the type of adsorption can be defined as physical adsorption. [25]

2.6. Kinetic Models

It is necessary to identify the types of adsorption mechanism in a given system, there are several kinetic equations available for analyzing experimental sorption; the experimental models tested in the present work are Pseudo-first, Pseudo-second. Intraparticle diffusion, Elovich and Bangham's models are also verified for studying the mechanism of diffusion.

2.6.1. Pseudo-First-Order Model

The adsorption kinetic data were described by the Lagergren pseudo-first-order model, which is the earliest known equation describing the adsorption rate based on the adsorption capacity. The Lagergren equation is commonly expresses as:

$$\frac{dq_t}{dt} = K_1(q_e - q_t) \qquad (15)$$

Where q_e and q_t are the adsorption capacity at equilibrium and at time t, respectively (mg/g), k_1 is the rate constant of pseudo-first order adsorption (l/min). By integration, it is found that [26]:

$$\ln(q_e - q_t) = \ln(q_e) - k_1(T)t \qquad (16)$$

2.6.2. Pseudo-Second-Order Model

The adsorption kinetic may be described by the pseudo-second order model, which is generally given as in:

$$\frac{dq_t}{dt} = k_2(t)(q_e - q_t)^2 \qquad (17)$$

Where k_2 (g/mg.min) is the corresponding rate constant of adsorption. By integration, the last equation simplified and can be rearranged and linearized to obtain the following relationship [27]:

$$\frac{t}{q_t} = \frac{1}{(k_2 \times q_e^2)} + \frac{t}{q_e} \qquad (18)$$

The second-order rate constants is used to calculate the initial sorption rate h (mg/g.min) given by

$$h = k_2 \times q_e^2 \qquad (19)$$

2.6.3. Elovich Model

The Elovich equation is one of the most useful models for describing chemisorption, which is given as [28]:

$$\frac{dq_t}{dt} = \alpha \exp(-\beta q_t) \qquad (20)$$

Where α represents the initial adsorption rate (mg/g.min) and β is related to the extent of surface coverage and activation energy for chemisorption (g/mg), they can be computed from the slope and intercept of the linear plot of qt versus ln(t) as shown as the linear equation of this model:

$$q_t = \frac{1}{\beta}\ln(\alpha\beta) + \frac{1}{\beta}\ln(t) \qquad (21)$$

2.6.4. Intraparticle diffusion Model

Adsorption is a multi-step process involving transport of the adsorbate (dye) molecules from the aqueous phase to the surface of the solid particles then followed by diffusion of the solute molecules into the pore interiors. The intraparticle diffusion is another kinetic model developed by Weber and Morris should be used to study the rate-limiting step for MB adsorption onto TES. If the experiment is a batch system with rapid stirring, there is a possibility that the transport of sorbate from solution into pores of the adsorbent is the rate-controlling step. The intra-particle diffusion is commonly expressed by [29]:

$$q_t = K_{dif}(t)^{1/2} + C \qquad (22)$$

Where K_{dif} (mg/gmin$^{1/2}$) is the intraparticle diffusion rate constant and C (mg/g) gives an idea about the thichness of the boundary layer.

2.6.5. Bangham's Model

It is generally expressed as [30]:

$$\log(\frac{C_0}{C_0 - q_t m}) = \log(\frac{k_0 m}{2.303\,V}) + \alpha \log(t) \qquad (23)$$

Where C_0 is the initial concentration of the adsorbate in solution (mg/l), V the volume of the solution (ml), m the weight of adsorbent used per liter of solution (g/l), q_t(mg/g) the amount of adsorbate retained at time t. α and k_0 are the constants of the model obtained by $\log[C_0 / (C_0 - mq_t)] = f(\log t)$ curves.

2.7. Adsorption Thermodynamics

To investigate the adsorption processes, the changes of thermodynamic parameters, such as, entropy ΔS°, enthalpy ΔH° and the Gibbs energy ΔG° and activation energy E_a for the system MB/TES must be determined. They can be calculated according to [31]:

$$\ln K_d = -\frac{\Delta H°}{RT} + \frac{\Delta S°}{R} \qquad (24)$$

$$K_d = \frac{q_e}{C_e} \qquad (25)$$

$$\Delta G° = -RT \ln(K_d) \qquad (26)$$

Where T(°C) is the absolute temperature, R is the universal gas constant and K_d (L/mol) is the distribution coefficient. ΔH and ΔS can be respectively calculated from the slope and intercept of the plot of ln(K_d) versus 1/T.

2.8. Sorption experiments in fixed-bed technique
2.8.1. Experimental Procedures

The fixed bed experiments were carried out in a glass column of 2 cm internal diameter, 30 cm of the length height and three sampling points at 5 cm intervals. A known quantity of the prepared activated carbon TES was packed in the column to yield the desired bed height of the adsorbent 50, 100 and 150 mm with a layer of glass wool at the bottom. Distilled water was passed through the column in order to remove impurities from the adsorbent. Three flow rates (2, 4 and 6 mL/min) were pumped to the top of the packed column by using peristaltic pump with different initial dye concentrations (5, 30, 50, 80 mg/L). The samples of AO7 solutions at the outlet of the column were taken at regular time intervals and the concentration of dye was measured using an UV–visible spectrophotometer at wavelength of 485 nm. Fixed bed studies were terminated when the column reached exhaustion [32]. The experimental detail of fixed bed column used in adsorption study is given in Table1. Briefly, the experiment was carried out by passing through column with controlled flow rate during experiments.

Table 1: Experimental details for column adsorption of ao7 onto TES

SYSTEM		Flow rate (mL/min)	[AO7] (ppm)	Bed height (cm)
	Flow rate	2, 4 and 6	30	15
	Initial Concentration	15	10, 30 and 50	15
	Bed height	15	30	5, 10 and 15

2.8.2. Response surface methodology

Response surface methodology is an experimental technique used for predicting and modeling complicated relation between independent factors and one or more responses.

In this study, response surface methodology was applied to optimize the adsorption of Acid orange 7 by TES. Experiments were performed using Box– Behnken design (BBD) . The second-order polynomial equation extended with additional cubic effects was employed as an objective function. The second order model is usually sufficient for the modeling and optimization on the basis of designs, however third order and higher effects are sometimes important, especially in order to achieve better fit and insignificant lack-of-fit. For instance, Box–Behnken design was created to estimate the second-order model, however there may be situations in which non- random portion of this model provides an inadequate representation of the true mean response, an indication of lack-of-fit of the second- order model. Thus, in this study some third order model terms were added to the second order polynomial equation. Accuracy of model fitting was evaluated by means of ANOVA. All calculations were performed in Statgraphics [33].

2.8.3. Box–Behnken design

In this study, the BBD design methodology was employed to optimize the operational variables and was used to predict impacts of respective parameters on the adsorption process. Among many factors affecting the adsorption process, three process variables , i.e. initial AO7 dye concentration (X_1), bed height (X_2) and flow rate (X_3) were selected and were considered as independent variables and the removal of dye (Y) as a response was defined and modeled. BBD contains set of 15 experiment runs whose values of each factor with three levels (low, medium, high), being is coded to standard values (-1, 0,+1) in the appropriate range and levels of parameters were listed in (Table 2). The second-order polynomial response equation was used to probe the interaction between the dependent and independent variables. The removal (%) of dye is selected as the response for the combination of independent variables, Subsequently experimental data was fitted to the second order polynomial model extended with additional cubic interaction effects (Eq. (27)) using the least square procedure as follows:

$$Y = b_0 + b_1 x_1 + b_2 x_2 + b_3 x_3 + b_{11} x_1^2 + b_{12} x_1 x_2 + b_{13} x_1 x_3 + b_{22} x_2^2 + b_{23} x_2 x_3 + b_{33} x_3^2 + e \quad (27)$$

where y is the predicted response associated with each factor level combination; The coefficients in the equation represent: the intercept (b_0) is constant, the main (b1,b2, b3) are linear effect, quadratic effect (b_{11}, b_{22}, b_{33}) and interactions (b_{12}, b_{23}, b_{13}) effects, respectively; xi and xj are the coded values of independent variables; and e is the residual error. Validation of the model fit and significance analysis of variables were performed using analysis of variance (ANOVA). The results were analyzed by analysis of variance (ANOVA) and a calculation correlation coefficient (R^2) between predicted and experimental points [34].

2.8.4. Model validation and optimization

Validation set was employed to explore the predication performance of the developed model. Moreover, the optimization process variables were obtained for the AO7system based on the D-optimality index in the Statgraphics software. The least square method was used to calculate the model coefficients through Eq. (3) using the Statgraphics software (version 4.2). To evaluate the statistical significance, ANOVA analysis (R^2, adjusted R^2, F-test and t-test), normal plots and residuals analysis were employed. The significance of the regression coefficients was appraised by the F and Student's t tests at the confidence level of 95% [35].

2.8.5. Experimental design

To determine the optimal conditions for the main parameters, a Box–Behnken design (BBD) was applied. For the adsorption process, significant variables, such as the initial dye concentration, flow rate, and bed height were regarded as the independent variables and designated as X_1–X_3, respectively. The dye concentration (X_1) range of 10–50 mg/L, flow rate (X_2) range of 2–6 ml/min, bed height (X_3) of 5–20 cm were chosen as given in Table 2.

Table 2: Independent process variables and their experimental levels used for Box–Behneken Design (BBD).

Variables, unit	Factors		Levels	
	X	-1	0	+1
Initial dye concentrations of AO7 (mg/L)	X_1	10	30	50
Bed height (cm)	X_2	5	10	15
Flow rate (ml/min) X_3	X_3	2	4	6

2.8.6. Selection of the significant parameters

The Box–Behnken design consists of 15 experimental points. The experimental conditions and the adsorption capacity obtained for each point set by the Box– Behnken design are shown in Table 3 (1–11), together with the three central point repetitions (12–15). The relationship between responses and processed variables was examined for the response approximation function (Y) using Eq. (27), following by the statistical analysis of the model obtained. The most significant process variables were identified by Box–Behnken design (BBD) experimental design. The advantage of this design is its ability to investigate of a large number of factors in a relatively low number of experimental runs. In this study 15 run BBD with 3 factors, including AO7 dye concentration (X_1), flow rate (X_2) and bed height (X_3) was considered. Each independent variable was tested at two levels, high and low, which were -1 and +1, respectively. All experiments were conducted in duplicate and the average values of removal dye were taken as a response (Y). The matrix design is shown in Table 3. On the basis of BBD three the most significant parameters were chosen for further investigation (modeling and optimization by RSM).

Table 3: Box–Behnken Design matrix with coded and uncoded values of the independent variables influencing adsorption of .AO7 by TES.

	Coded values (uncoded values)		
Experimental run No.	X_1 [ppm]	X_2 [cm]	X_3 [ml/min]
1	1 (50)	0 (10)	-1 (2)
2	0 (30)	0 (10)	0 (2)
3	0 (30)	0 (10)	0 (2)
4	0 (30)	-1 (5)	1 (6)
5	0 (30)	-1 (5)	-1 (2)
6	-1 (10)	0 (10)	1 (6)
7	0 (30)	1 (15)	1 (6)
8	1 (50)	0 (10)	1 (6)
9	-1 (10)	1 (15)	0 (2)
10	1 (50)	1 (15)	0 (2)
11	-1 (10)	-1 (5)	0 (4)
12	-1 (10)	0 (10)	-1 (2)
13	0 (30)	1 (15)	-1 (2)
14	0 (30)	0 (10)	0 (2)
15	1 (50)	-1 (5)	0 (2)

2.8.7. Analysis of variance (ANOVA)

ANOVA expounds every variation in the statistically obtained model and importance of each model parameters. The significance of the model was evaluated by F-test for a confidence level of 95% as well as lack-of-fit test. In general, the greater the F-value and the smaller the p-value, the more significant is a model. Moreover, effects and their importance in the model were investigated adapting t-test and p-value. Usually, the larger the t-value and lower probability p-value (p < 95%), the model parameter is considered as significant [36].The sum of squares, degree of freedom and mean squares were also determined for the model and error.

3. Results and discussion

3.1. FTIR and DRX Spectral Analysis

Analysis of FT-IR spectrum of TES biosorbent in the range of 400 – 4000 cm^{-1} as shown in Fig.2.-a- shows some bands at 3520 cm^{-1} that are assigned to –OH stretching mode vibrations due to inter-and intra-molecular

hydrogen bonding of polymeric compounds. The peak at 1638cm^{-1} is due to asymmetric stretching vibrations of C=O and the peak observed at 1525cm^{-1} can be assigned to aromatic compound group and the stretching and folding of carbonate group has been assigned to peaks at 1500 cm^{-1} and 865 cm^{-1}.The X-ray diffraction of our biosorbent is shown in Fig.2.-b- .The figure shows a main peak appeared at 2Theta = 30. In addition, this spectrum shows several other small peaks at 2Theta = 22.78, 35.88, 40.28, 48, 49, 54.78, 62.58, 50.858, 57.488, 60.748 and 62. This spectrum confirms the presence of calcite.
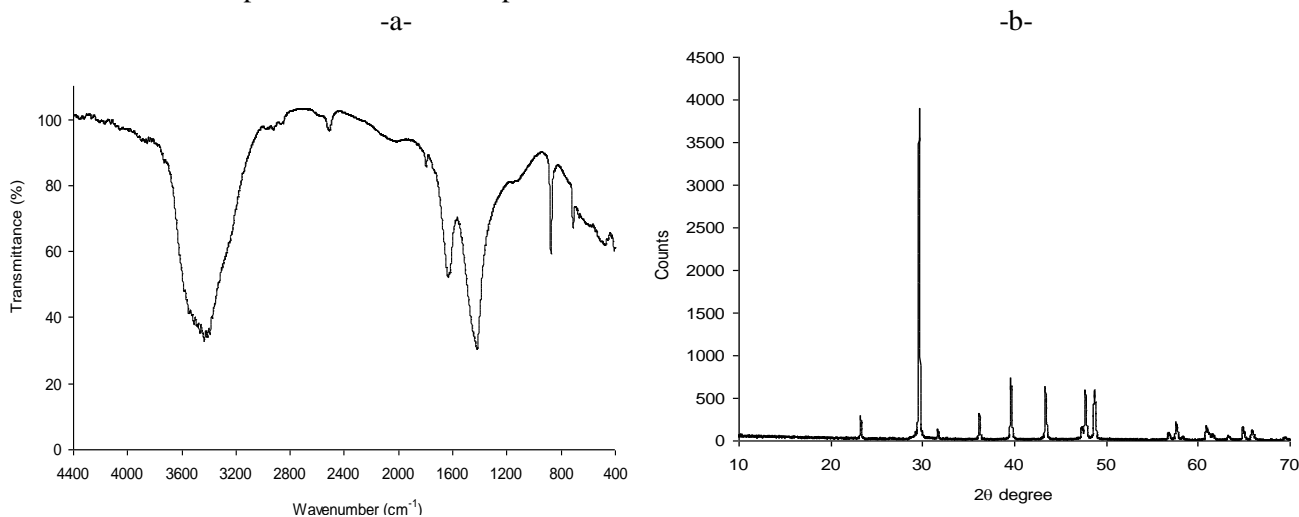

Fig.2: -a-FTIR spectra and -b-X-ray diffraction pattern of TES

3.2. Effect of Initial MB Concentration and Contact Time on MB Adsorption
To study the influence of concentration of the sorption of MB on TES, 3g TES added in each 3 liters of MB solution with initial concentrations (5–100 mg/L) at 25°C. The results obtained are shown in Fig. 3 and indicate that the uptake rate of MB dye adsorbed per gram of TES increases gradually at the beginning and after the adsorption of MB reached equilibrium at 100 min. We can say that the equilibrium time is independent of the concentration and the amount adsorbed at equilibrium increases with concentration from 5 to 62 mg/g, with increase in the initial MB concentration from 5 to 100 mg/L. This is because the diffusion of dye molecules from the solution to the adsorbent surface is accelerated by increasing the sorbate quantity.
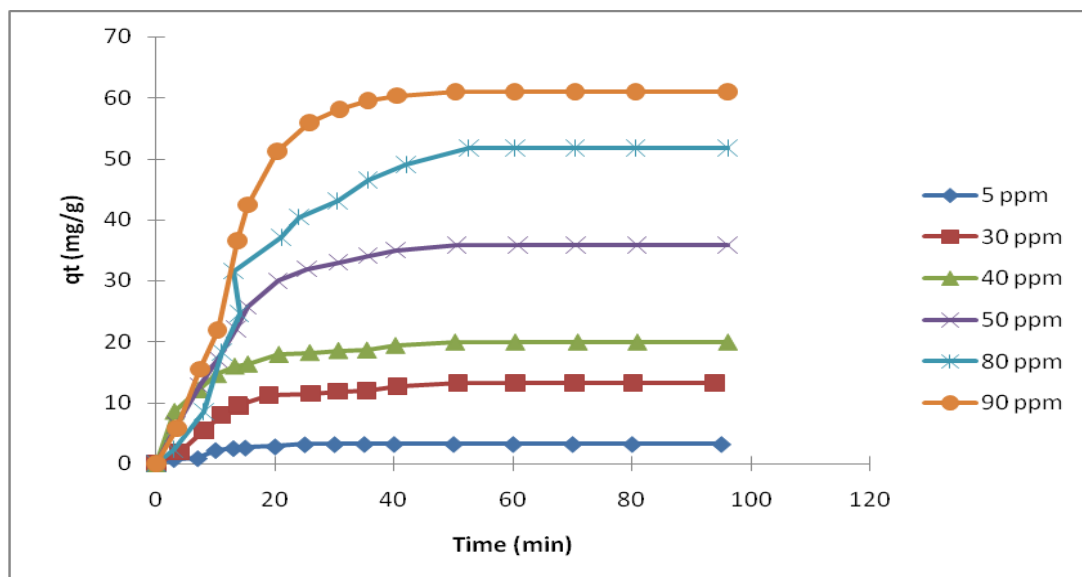

Fig. 3: Kinetics of MB adsorption by TES at different initial concentrations

3.3. Effect of Temperature
To determine the effect of temperature on the biosorption of the MB dye, experiments were conducted at 20, 25, 30 and 35°C. The experiments were performed by adding 1 g/l of TES to the MB solution at a fixed concentration (80 ppm) and constant pH. Fig.4 shows that the equilibrium uptake percentage of MB dye ions using TES was affected by temperature, it decreased with an increase in temperature, and it's due to the

decrease of the physical forces responsible for sorption. Furthermore, the decrease uptake of the cationic MB dye removal at higher temperatures (above 20°C) may be attributed to the destruction of some polymeric active sites on the adsorbent surface due to bond rupture, as well as the deformation of surfaces at higher temperatures. Consequently, the study found that the optimum working range was 20°C.
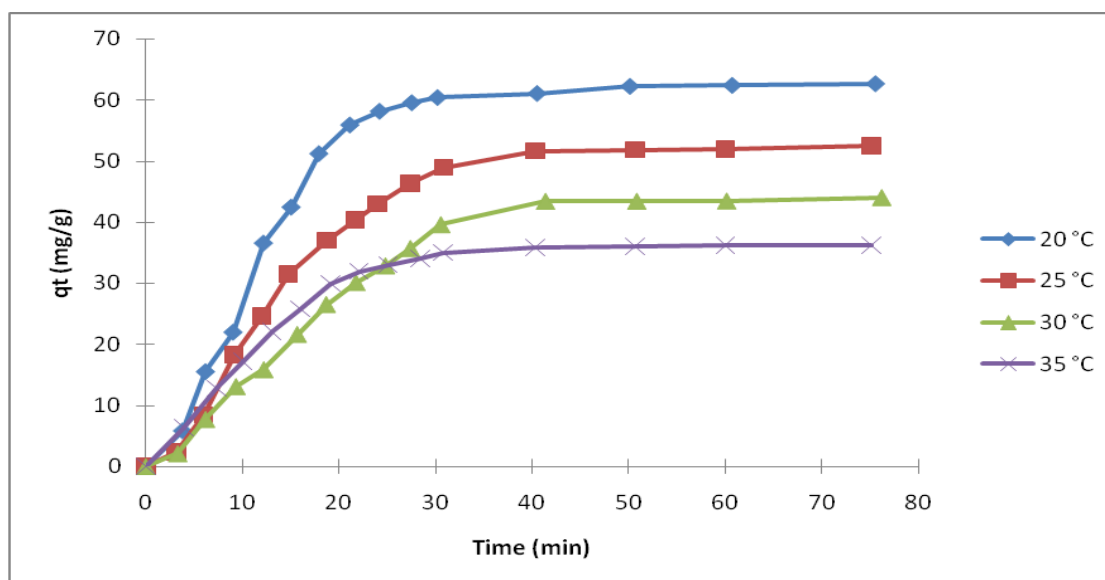

Fig. 4: Effect of temperature on the adsorption of MB

3.4. Isotherm Modeling of the Sorption Equilibrium Depending on Temperature

Analysis of the isotherm data is important to develop equations that correctly represent the results and could be used for design purposes. Table 4 shows the fitting parameters for the measured isotherm data for MB adsorption onto TES on the linear forms of Langmuir, Freundlich, Dubinin–Radushkevich(D–R), generalized isotherm and Temkin isotherms were simulated.

Table 4: Comparison of the Coefficients Isotherms Parameters for MB Adsorption onto TES

Models	Temperature(°C)			
	20	25	30	35
Langmuir 1				
Q_m(mg/g)	200	175.439	178.571	140.845
$10^2.K_1$(l/mg)	5.241	5.572	4.338	6.532
R^2	0.9985	0.9992	0.9994	0.9958
Freundlich				
K_f	24.264	33.205	27.292	46.619
N	2.2422	2.9860	2.7056	4.8972
R^2	0.936	0.9722	0.9643	0.9928
Temkin				
k_1	0.4526	0.6366	0.4225	2.4965
B_1	45.214	36.418	39.078	21.687
b_1	3.6776	5.7073	6.3826	13.418
R^2	0.9923	0.9965	0.9912	0.9836
(D-R)				
Q_m(mg.g^{-1})	130.843	135.233	126.723	114.206
K(mol^2/kJ^2)	0.002	0.003	0.004	0.003
E(kJ/mol)	15.811	12.910	11.180	12.910
R^2	0.932	0.971	0.956	0.978

The results obtained from the form of Langmuir model for the removal of MB onto TES are showed in Table 4. It can be observed that the adsorption isotherm of MB onto TES fits Langmuir isotherm well with higher

correlation coefficients (R^2) in comparison with other isotherms, reflecting that the adsorption sites on the surface of TES are evenly distributed. According to Langmuir adsorption isotherm, the Q_{max} for MB are calculated to be 200, 175.44, 178.57 and 140.85 mg.g^{-1} at 20, 25 , 30 and 35°C respectively. We can see from the table 4 that the increase in temperature leads to a decrease in the adsorbed amount, it can be said that the low temperatures are of most interest and the maximum monolayer capacity Q_m adsorbed at 20°C is 200 mg /g obtained from Langmuir model. The maximum adsorption of MB on TES decreases with increasing the temperature, exhibiting the exothermic nature of the adsorption process.

Freundlich constants can be determined from the plot of log (q_e) versus log (C_e). Thus we can generate the value of K_F from the intercept and 1/n from the slope. The correlation coefficients, $R^2 > 0.93$, obtained in Table 4.Freundlich model is comparable to that obtained from Langmuir model linear form. This result indicates that the experimental data fitted well Freundlich model. The values of n_F are higher than unity, indicating that adsorption of MB onto TES is a favorable process.

The Temkin constants K_1 and B_1 are calculated from the slope and the intercept of q_e versus ln(C_e). The linear isotherm constants and coefficients of determination are presented in Table 4. Examination of the data shows that the Temkin isotherm is applicable to the MB adsorption onto TES judged by high correlation coefficient (R^2) 0.992, 0.996, 0.991 and 0.983.

In the D–R model, the plot of ln (q_e) versus ε^2 gives K ($mol^2/(kJ^2)$) and the adsorption capacity, Q_m(mg/g). The constant K gives the mean free energy of adsorption (E) per molecule of the sorbate when it is transferred to the surface of the solid from infinity in the solution. Calculated D–R constants for the adsorption of MB on TES were given in Table 4. The value of regression coefficient of D-R isotherm R^2 are 0.932, 0.971, 0.956 and 0.978 is lower than the Langmuir value and the Freundlich value, in this case, D–R equation represents the poorer fit of experimental data than the other isotherm equations. According to the calculated E as 15.811,12.910,11.180 and 12.910kJ/mol respectively at 20, 25, 30 and 35°C, which are between 8 and 16 kJ/mol, the type of adsorption of MB on the TES was described as chemical adsorption.

The separation factor R_L values for the sorption of MB dye on the eggshell biosorbent have been shown in Table 5. All R_L values fall between zero and one; this fact supports the previous observation where the Langmuir isotherm was favorable for dye sorption for all studied temperatures.

Table 5: Dimensionless Separation Factor (R_L) at Different Initial Dye Concentrations Studied at Different Solution Temperatures for the Sorption of MB Dye onto the TES Biosorbent

C (mg/l)	T (°C)			
	20	25	30	35
10	0.65612	0.64219	0.69746	0.60490
20	0.48823	0.47295	0.53546	0.43359
40	0.32295	0.30972	0.36562	0.27680
60	0.24128	0.23025	0.27758	0.20329
80	0.19257	0.18324	0.22371	0.16063
100	0.16023	0.15216	0.187346	0.13277

3.5. Kinetic models

The biosorption data were analyzed according to the pseudo first- order kinetic model by the plot of ln($q_e - q_t$) versus t. According to Fig.5, we see that the first order kinetic model is not checked for all temperatures because the curves are not perfectly linear with $R^2 < 0.98$. Furthermore, the table III shows that the calculated q_e values are too low compared with experimental q_e values. It is therefore imperative to check the second order model.

The plots of t/q_t versus t give straight lines at different temperatures as showed in Fig.6 with high values of R^2 which are greater than 0.98. Therefore, that confirms the applicability of the pseudo-second order equation. Values of the rate constant k_2 and equilibrium adsorption capacity q_e were calculated from the intercept and slope of the plots of t/qt versus t, respectively.

All parameters are summarized in Table 6which shows better results for the pseudo second order model than the pseudo first order. Practically, the increase in temperature from 20 to 35°C is accompanied by a decrease of q_e from 66.67 to 40 mg/g respectively. However, the results obtained using the pseudo-second-order model are not enough to predict the diffusion mechanism.
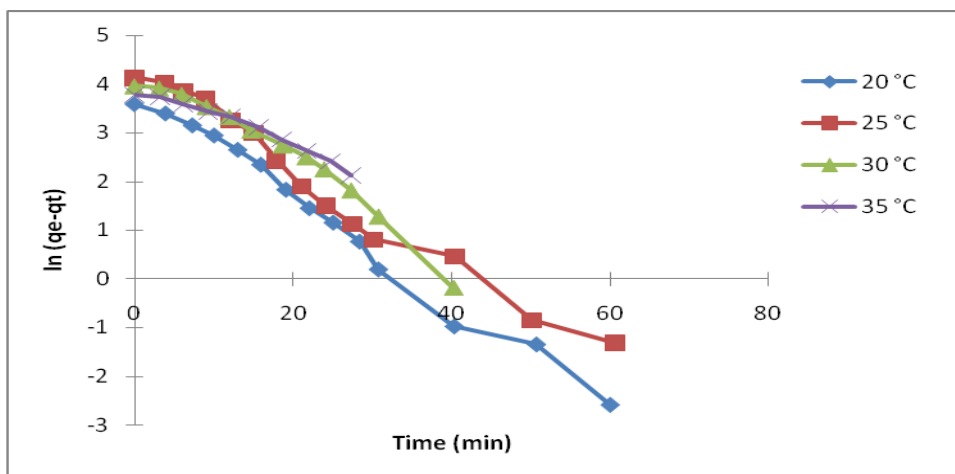
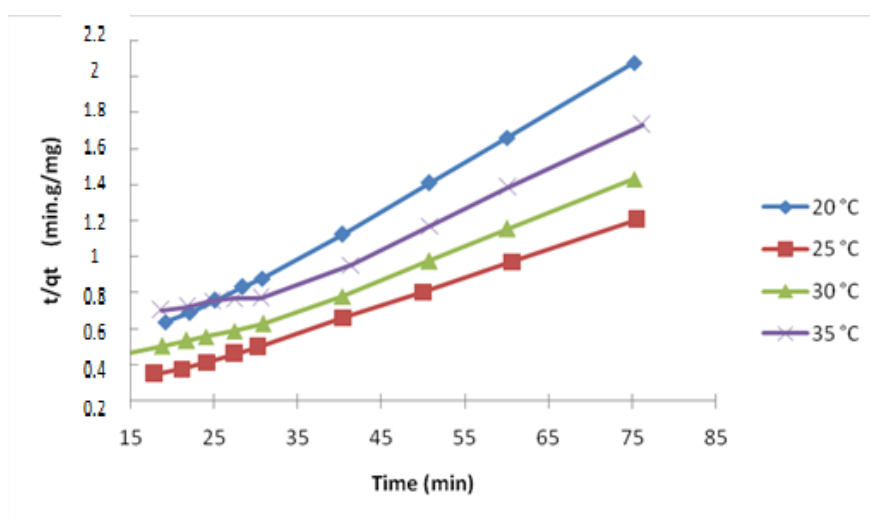**Fig.5:** Pseudo-first-order kinetics for methylene blue adsorption onto eggshell at different temperature

Fig.6: Plot of the pseudo-second-order model at different initial MB temperatures (20 - 35 °C)

Table 6: Comparison of the First- and Second-Order Adsorption Rate Constants and q_e Values for Different MB Temperature and TES

T(°C)		Pseudo 1st order				Pseudo second order		
		R_1^2				$10^{-3}.k_2$	H	q_e
	q_{exp} (mg/g)		k_1 (l/min)	q_e (mg/g)	R_2^2	(g/mg min)	(mg/g.min),	(mg/g)
20	62.56	0.97	0.099	71.02	0.998	4.09	18.182	66.67
25	52.55	0.95	0.099	80.96	0.988	1.47	5.747	62.5
30	44	0.96	0.061	52.03	0.975	1.132	3.496	55.56
35	36.22	0.98	0.108	47.56	0.998	5.787	9.259	40

The Elovich parameters α and β can be computed from the slope and intercept of the linear plot of q_t versus ln t, they are reported in Table 7.

The intraparticle diffusion is another kinetic model developed by Weber and Morris that should be used to study the rate-limiting step for MB adsorption onto TES. The intraparticle diffusion is the sole rate-limiting step if q_t versus $t^{1/2}$ plots pass through the origin, which is not the case in Fig.7 It may be concluded that surface adsorption and intraparticle diffusion were concurrently operating during the methylene blue eggshell interactions. The values of k_{diff1} and k_{diff2} as obtained from the slopes of the two straight lines are listed in Table 7. The intraparticle diffusion rate constant K_{dif1} were in the range of 0.358–1.181mg/gmin$^{1/2}$ and it increases with an increase of temperature.

Table 7: The Parameters Obtained from Elovich Kinetics Model and Intraparticle Diffusion Model Using Different Eggshells Temperatures

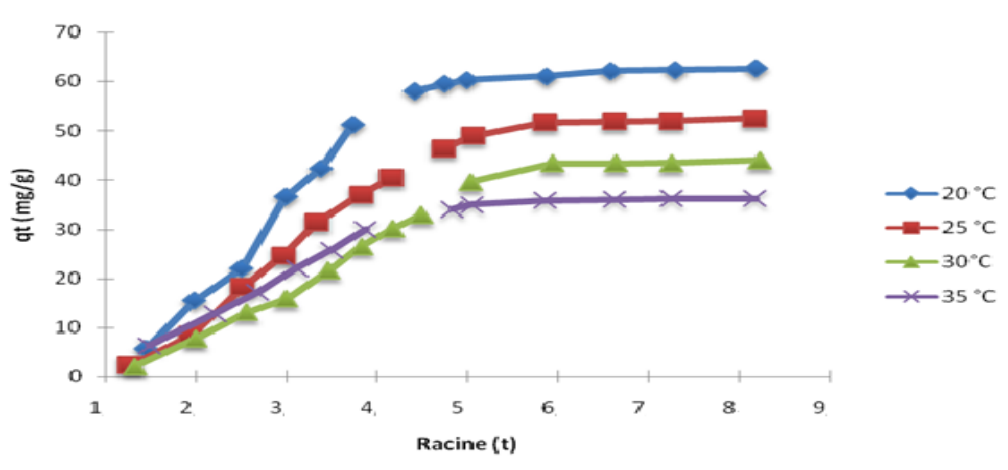|	Temperature			
	20°C	25°C	30°C	35°C
Elovich				
$10^2 . \beta$ (g/mg)	6.16	3.44	4.64	5.71
α (mg/g min)	4.899	8.409	6.279	4.546
R^2	0.987	0.978	0.98	0.959
Intraparticlediffusion				
Kdiff1	0.358	0.884	0.981	1.181
C	33.29	55.3	44.46	34.35
R^2	0.786	0.9	0.709	0.644
Extraparticle diffusion				
Kdiff2	9.006	19.62	13.87	9.928
C	-10.51	-33.48	-23.38	-16.98
R^2	0.99	0.99	0.992	0.992
Bangham				
k_0(mL/g/L)	27.752	0.3519	16.232	26.448
α	-1.355	2.803	1.175	0.851
R^2	0.897	0.971	0.975	0.983

Fig.7: Intraparticle diffusion model plot for the adsorption of MB onto TES at different initial temperatures

For intraparticle diffusion plots, the first, sharper region is the instantaneous adsorption or external surface adsorption that can be attributed to the film diffusion. The second region is the gradual adsorption stage where intraparticle diffusion is the rate limiting. It confirms that intraparticle diffusion was not the only rate limiting mechanism in the sorption process. Table 7 lists the kinetic constants α and k_0 obtained from the Bangham's equation by plotting $log[C_0/(C_0-mq_t)]$ against log t. Thus, when temperature passed from 20 to 35°C. the value of α increased from -1.355 to 0.851 and the value of k_0 decreased from 27.752to 26.448 (mL/g/L). The experimental data did not give a good correlation. In addition, it was found that the correlation coefficients for the Elovich model are higher than those obtained for Bangham's model. This result still confirmed that the pore diffusion is not the only rate-controlling step.

3.6. Thermodynamic Parameters of Adsorption
In adsorption processes, thermodynamic parameters are the actual indicators for practical application. The values of $\Delta H°$ and $\Delta S°$ were determined from the slope and the intercept of the plot of lnK_d versus $1/T$.As shown in table 8, the negative value of $\Delta H°$ (-30.2297 kJ/mol) shows that the adsorption is exothermic as process. The negative value of $\Delta S°$ (-0.0981kJ/mol.°C) indicate that there a reduction of disorder in the solid/solution interface during the adsorption process. The negative values of $\Delta G°$ that increased from -1.4605kJ/mol to -0.4786kJ/mol with an increase in temperature from 20°C to 30 °C indicate the spontaneous nature of this biosorption that the adsorption is more favorable at low temperatures.

Table 8: Thermodynamic Parameters Obtained from Isotherm Adsorption of MB onto TES

T (°C)	K_d (L/mg)	$Ln(K_d)$	ΔG (kJ/mol)	ΔH (kJ/mol)	ΔS (J/mol.°C)
20	1.8007	0.58817	-1.4605	-30.230	-98.188
25	1.4160	0.34781	-0.9696		
30	1.2964	0.25955	-0.4786		
35	0.9466	-0.05487	0.0123		

3.7. Response Surface Methodology: Box–Behnken Design

Response surface methodology (RSM) is more advantageous than the traditional single parameter optimization because it can save time, space and raw material. In experimental design, a Box– Behnken design (BBD) is a type of RSM, and it is used for optimizing the important process variables. The most important parameters, which affect the efficiency of adsorption of AO7 onto TES, are AO7 dye concentration, flow rate and bed height of the solution in a continuous fixed bed. In order to study the combined effect of these factors, experiments are performed for different combinations of the physical parameters using statistically designed experiments. The initial dye concentration range studied is between 10 and 50 ppm. The flow rate is between 2 and 6 ml/min. The bed height is varied between 5 and 20 cm .The main effects of each of the parameter on AO7 removal efficiency is given in Fig.8. Fig. 8 shows that the removal efficiency increases with increasing AO7 dye concentration and bed height and with decreasing flow rate. Consequently, we note high AO7 removal efficiencies at high initial dye concentration.
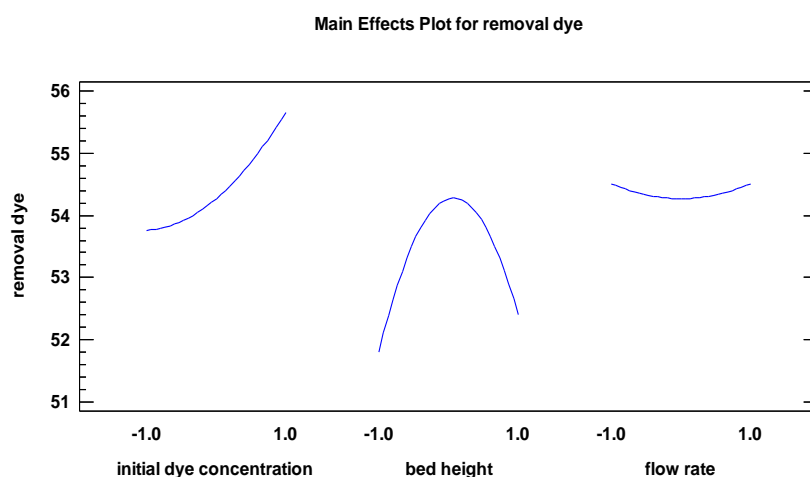

Fig.8. Main effects plot of parameters for AO7 removal efficiency.

Table 9 shows the experimental results of removal of AO7 in the solution for the 15 experiments. Using the experimental results, the regression model equations (second-order polynomial) relating the response is developed and is given in Eqs. (27). Apart from the linear effect of the parameter for the response, the RSM also gives an insight into the quadratic and interaction effect of the parameters. These analyses are done by means of Fisher's 'F' test and Student 't' test. The Fisher's 'F' test is used to determine the significance of each of the interaction among the variables, which inturns may indicate the patterns of the interactions among the variables. In general, the larger the magnitude of F, the smaller the value of P, the more significant is the corresponding coefficient term. The regression coefficient, F and P values for all the linear, quadratic and interaction effects of the parameter are given in Table 10for the removal of AO7. It is observed that the coefficients for the linear effect of the factors initial dye concentration (p=0.0316) for the response is significant except flow rate and bed height (P =1.000 and p=0.3932) for removal of dye is slightly less significant. However, for the removal efficiency of AO7, the interaction effect of the variables dye concentration and bed height is found highly significant p=0.007 exempt the interaction between dye concentration and flow rate (P = 0.0688).
Consequently, the best fitting response function, for the AO7 removal efficiency model are then conveniently written as follows:

$$Y = 54.2667 + 0.95x_1 + 0.3x_2 + 0.4416x_1^2 + 0.95x_1x_2 - 1.05x_1x_3 - 2.1583x_2^2 - 0.65x_2x_3 + 0.2416x_3^2 \ (28)$$

Where Y (%) is the removal dye of AO7 ; x_1, x_2 and x_3 are the AO7 dye concentration , flow rate and bed height respectively.

Table 9: The experimental data for ao7 removal efficiency in solution according to BBD.

Experimental run No.	Removal dye Y [(%)]	
	Experimental values	Predicted responses
1	56.00	56.95
2	54.20	54.26
3	54.30	54.26
4	52.00	52.70
5	51.60	51.40
6	56.00	55.05
7	51.80	52.00
8	54.80	54.85
9	50.20	50.95
10	55.00	54.75
11	52.00	52.25
12	53.00	52.95
13	54.00	53.30
14	54.30	54.26
15	53.00	52.25

Table 10: Analysis of variance and corresponding f and p values for AO7 removal efficiency.

Source	Sum of Squares	Df	Mean Square	F-Ratio	P-Value
A:intial concentration	7.22	1	7.22	8.75	0.0316
B:bed height	0.72	1	0.72	0.87	0.3932
C:flow rate	0.00	1	0.00	0.00	1.0000
AA	0.720256	1	0.720256	0.87	0.3931
AB	3.61	1	3.61	4.37	0.007
AC	4.41	1	4.41	5.34	0.0688
BB	17.2003	1	17.2003	20.84	0.0060
BC	1.69	1	1.69	2.05	0.2118
CC	0.215641	1	0.215641	0.26	0.6310
Total error	4.12667	5	0.825333		
Total (corr.)	40.844	14			

The ANOVA table partitions the variability in removal dye into separate pieces for each of the effects. It then tests the statistical significance of each effect by comparing the mean square against an estimate of the experimental error. In this case, 3 effects have P-values less than 0.05, indicating that they are significantly different from zero at the 95 % confidence level. The R-Squared statistic indicates that the model as fitted explains 89.8965% of the variability in removal dye. The adjusted R-squared statistic, which is more suitable for comparing models with different numbers of independent variables, is 71.7102 %. Further, the ANOVA for AO7 removal efficiency in solution indicates that the second-order polynomial model Eqs. (28) is highly significant and adequate to represent the actual relationship between the response and variables, with very a high value of coefficient of determination (R^2 = 0.8989for AO7 removal efficiency in solution. This implies that 89.89% of sample variation for AO7 removal efficiency in solution is explained by the model. The statistical significance of the ratio of mean square variation due to regression and mean square residual error is tested using ANOVA. ANOVA is a statistical technique that subdivides the total variation in a set of data into component parts associated with specific sources of variation for the model. According to the ANOVA (Table 10), the $F_{statistics}$ values for all regression are higher. The large value of F indicates that most of the variation in the response can be explained by the regression equation. The associated P valueis used to estimate whether $F_{statistics}$ is large enough to indicate statistical significance. The ANOVA table also shows a term for residual error, which measures the amount of variation in the response data left unexplained by the model. The form of the model chosen to explain the relationship between the factors and the response is correct. The 3D response

surface and 2D contour plot are generally the graphical representation of the regression equation. We will use it to search the optimal values of the process parameters. Then, the response surface plots and contour plots to estimate the removal efficiency (Figs. 9 and 10) is given.
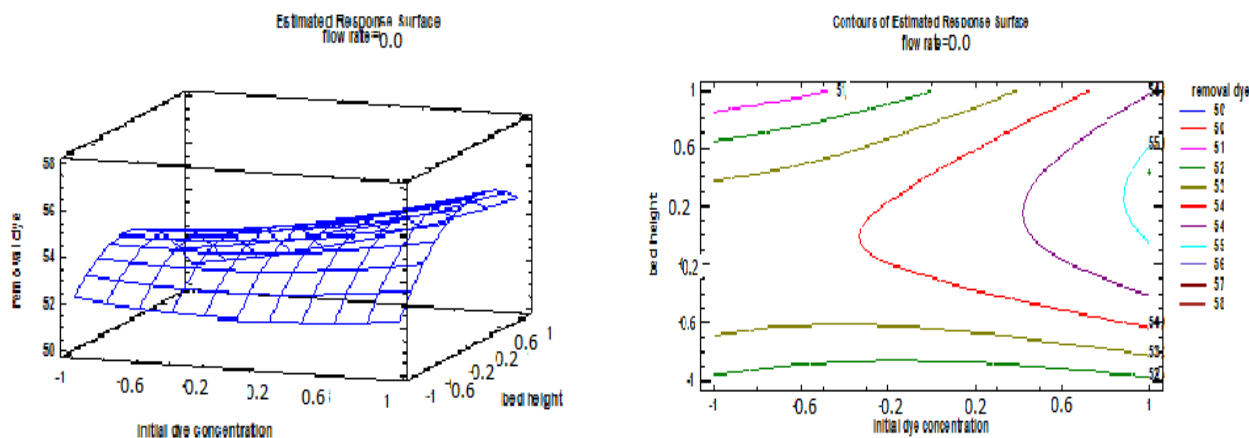

Fig.9. Response surface plot of AO7 removal efficiency.**Fig.10.**Contour plot of estimated response surface of AO7 removal efficiency.

Thus, the surface and contour plots for AO7 removal efficiency in Fig. 10 shows the interaction effect of bed height and initial concentration .The response surface of mutual interactions between the variables is found to be elliptical and the maximum AO7 removal efficiency is obtained in the following cases: The bed height and initial concentration increase simultaneously. The initial concentration increases and the bed height are between 10 and 15 cm and remain unchanged. The bed height increases and initial concentration is between 10 and 20 ppm and remains stable. The geometrical representation of the response removal dye , when the bed height and initial concentration increases the removal dye increases. We also note that, the influence of flow rate is not significant. Then, to have a good removal dye it is beneficial to work with high bed height of column. The highest value of the bed height which gives maximum of AO7 removal is 15 cm.

Conclusions

In this study, we have investigated the efficiency of Eggshell treated by NaOH (TES) in removing the cationic dye methylene blue (MB) andanionic dye AO7 from aqueous solution. In batch study TES could almost remove over 75% of MB within 100 min contact time; The equilibrium time is independent of the initial concentration of the solution and the amount adsorbed at equilibrium increases with concentration, this is because the diffusion of dye molecules from the solution to the surface of the adsorbent is accelerated by increasing the dye concentration. The adsorbed amount decreases with increasing temperature. Results indicate also that the adsorption isotherm data were fitted good agreement with the Langmuir isotherm models by comparing the values of the linear correlation coefficient R^2, the adsorption capacity was found to be 200 mg.g^{-1} at 20°c. The adsorption process followed pseudo-second order kinetics and was spontaneous and exothermic; furthermore, the intraparticle diffusion was not the only rate limiting mechanism in the sorption process. The continuous study clearly demonstrated the applicability of adsorption process using the fixed bed for AO7 removal. This study clearly showed that RSM is one of the suitable methods to optimize the best operating conditions to maximize the AO7 removal. BB design is successfully employed for experimental design and analysis of results. The TES, which was used without further purification for the removals of AO7 from aqueous solution because it leans, close to practical purposes. The process variables of removal of dye by TES have been optimized based on RSM method and the individual and interaction effects of the process variables were investigated. The results indicated that all the three process variables have a direct relationship for the removal AO7 dye onto TES. Satisfactory empirical model equations are developed for the removal of AO7 in solution using RSM to optimize the parameters. Graphical response surface and contour plot is used to locate the optimum point. This study shows that TES is an effective biosorbent for removal of anionic and cationic dyes from aqueous solutions.

References

1. Elkady M.F., Ibrahim A.M., El-Latif, M.A., *Desalin*. 278 (2011) 412–423.
2. Barka N., Assabbane A., Nounah A., Ichou Y.A., *J. Hazard. Mater.*152 (2008) 1054–1059.
3. Witoon T., *Ceramics International* 37 (2011) 3291–3298.
4. Barka N., Abdennouri M., Boussaoud A., Galadi A., Baâlala M., Bensitel M., Sadiq M., *Arab. J. Chem.* 7 (2014) 752–757.
5. Tsai W.T., Yang J.M., Lai C.W., Cheng Y.H., Lin C.C., Yeh C.W., *Bioresour. Technol*. 97 (2006) 488–493.
6. Köse T.E., Kıvanç B., *Chem. Eng. J.* 178 (2011) 34– 39.
7. Liu S.X., Qu Z.P., Han X.W., Sun C.L., *Catal. Today* 93 (2004) 877–884.
8. Danion A., Bordes C., Disdier J., Gauvrit J.Y., Guillard C., Lantéri P., Jaffrezic-Renault N. , *J. Photochem. Photobiol. Chem.* 168 (2004) 161–167.
9. Fernandez J., Kiwi J., Baeza J., Freer J., Lizama C., Mansilla H.D., *Appl.Catal. B Environ.* 48 (2004) 205– 211.
10. Lim L.B., Priyantha N., Tennakoon D.T.B., Chieng H.I., Dahri M.K., Suklueng M., *Arab.J. Chem.*(2014) .
11. El Boujaady H., El Rhilassi A., Bennani-Ziatni M., El Hamri R., Taitai A., Lacout J.L., *Desalin*. 275 (2011) 10–16.
12. Tsai W.T., Hsien K.J., Hsu H.C., Lin C.M., Lin K.Y., Chiu C.H., *Bioresour*. *Technol*. 99 (2008) 1623–1629.
13.Seid L., Chouder D., Maouche N., Bakas I., Barka N., *J. TaiwanInst. Chem.Eng*. 45 (2014) 2969–2974.
14. Pathania D., Sharma S., Singh P., *Arab. J. Chem.* (2013)205-217.
15. Daneshvar N., Aber S., Dorraji M.S., Khataee A.R., Rasoulifard M.H., *Sep. Purif. Technol.* 58 (2000) 91– 98.
16. Arami M., Limaee N.Y., Mahmoodi N.M., *Chem. Eng. J.* 139 (2008) 2–10.
17. Barka N., Assabbane A., Nounah A., Laanab L., Ichou Y.A., *Desalin*. 235 (2009) 264–275.
18. Gürses A., Hassani A., Kıranşan M., Açışlı Ö., Karaca S., *J. WaterProcessEng.* 2 (2014) 10–21.
19. Zheng W., Li X. M., Wang F., Yang Q., Deng P., Zeng G. M., *J. Hazard. Mater.* 157(2008), 490-495.
20. Gonte R., Balasubramanian K., *J. of SaudiChem. Soc.* (2013)75-84.
21. Slimani R., El Ouahabi I., Abidi F., El Haddad M., Regti A., Laamari M.R., Lazar S., *J. TaiwanInst. Chem. Eng*. 45 (2014) 1578–1587.
22. Aarfane A., Salhi A., El Krati M., Tahiri S., Monkade M., Lhadi E.K., Bensitel M., *J.Mater. Environ. Sci.* 5 (2014) 1927-1939.
23. Khaled A., El Nemr A., El-Sikaily A., Abdelwahab O., *J. Hazard. Mater.* 165 (2009) 100–110.
24. Köse T.E., Kıvanç B., *Chem. Eng. J.* 178 (2011) 34– 39.
25. Silva J.P., Sousa S., Rodrigues J., Antunes H., Porter J.J., Gonçalves I., Ferreira-Dias S. , *Sep. Purif. Technol.* 40 (2004) 309–315.
26. Meziti C., Boukerroui A., *Procedia Eng*. 33 (2012) 303 – 312.
27. Tan C.Y., Li M., Lin Y.M., Lu X.Q., Chen Z.L., *Desalin*. 266 (2011) 56–62.
28. Zewail T.M., Yousef N.S., *Alex.Eng. J.* 54 (2015) 83–90.
29. Elmoubarki R., Mahjoubi F.Z., Tounsadi H., Moustadraf J., Abdennouri M., Zouhri A., Barka N., *WaterResour. Indus.* 9 (2015) 16–29.
30. Mezenner N.Y., Bensmaili A. ,*Chem. Eng. J.* 147 (2009) 87–96.
31. Hassan W., Farooq U., Ahmad M., Athar M., Khan M.A., *Arab. J. Chem.* 4 (2013)78-87.
32. Lizama C., Freer J., Baeza J., Mansilla H.D., *Catal. Today* 76 (2002) 235–246.
33. Sakthivel S., Neppolian B., Shankar M.V., Arabindoo B., Palanichamy M., Murugesan V., *Sol. Energy Mater. Solar Cells* 77 (2003) 65–82.
34. Guimaraes J.R., Maniero M.G., Araujo, R.N., *J. Environ. Manage.* 110 (2012) 33–39.
35. Shu H.Y., Chang M.C., Fan H.J., *J. Hazard. Mater.* 118 (2005) 205-211.
36. Muruganandham M., Swaminathan M., *Sol. Energy Mater. Sol. Cells* 81 (2004) 439-457.

(2017) ; http://www.jmaterenvironsci.com/